Cytoplasmic incompatibility between Old and New World populations of a tramp ant

Çiğdem Ün[1°], Eva Schultner[1°], Alejandro Manzano-Marín[2], Laura V. Flórez[3], Bernhard Seifert[4], Jürgen Heinze[1], Jan Oettler[1*]

[1]Zoology/Evolutionary Biology, University of Regensburg, Universitätsstrasse 31, 93053 Regensburg, Germany

[2]Centre for Microbiology and Environmental Systems Science, University of Vienna, Althanstraße 14, 1090 Vienna, Austria

[3]Institute of Organismic and Molecular Evolution, Evolutionary Ecology Department, Johannes Gutenberg University Mainz, Hanns-Dieter-Hüsch-Weg-15, 55128 Mainz, Germany

[4] Senckenberg Museum of Natural History Görlitz, Am Museum 1, 02826 Görlitz, Germany

°contributed equally

*corresponding author:
Jan Oettler
joettler@gmail.com

Author ORCIDs:
Çiğdem Ün: 0000-0002-0817-3630
Eva Schultner: 0000-0002-5069-9732
Alejandro Manzano-Marín: 0000-0002-0707-9052
Laura V. Flórez: 0000-0002-0761-3729
Jürgen Heinze: 0000-0002-9403-5946
Jan Oettler: 0000-0002-8539-6029

Classification: Biological Sciences: Evolution

Key words: *Wolbachia*, social insects, speciation, endosymbiont, antibiotics

Contributions

CÜ performed the crosses and qPCR
ES analyzed and visualized the data
AMM assembled *Wolbachia* genomes, performed comparative genomic analyses, calculated the phylogeny and annotated CI genes
LVF conducted FISH analyses
BS revised the taxonomic status of the populations
JH acquired funding and reviewed and edited the manuscript
JO conceived and supervised the study
JO, ES and CÜ wrote the original draft of the manuscript
All authors revised and approved the final version of the manuscript

Abstract

As we enter the Anthropocene, the evolutionary dynamics of species will change drastically, and as yet unpredictably, due to human activity. Already today, increases in global human traffic have resulted in the rapid spread of species to new areas, leading to the formation of geographically isolated populations. These go on to evolve in allopatry, which can lead to reproductive isolation, and potentially, the formation of new species. Surprisingly, little is known about such eco-evolutionary processes in ants, even though numerous invasive ant species are globally distributed in geographically isolated populations. Here, we describe the first case of cytoplasmic incompatibility (CI) between populations of a cosmotropic distributed tramp ant with Asian roots, *Cardiocondyla obscurior*, which has acquired a novel *Wolbachia* strain in the New World. Our study uncovers the first symbiont-induced mechanism of reproductive isolation in ants, providing a novel perspective on the biology of globally distributed ants.

Introduction

Ants are the most abundant group of insects on earth, and numerous ant species are classified as highly invasive on a global scale. Their distribution is, on the one hand, strongly facilitated by humans. This is evidenced, for instance, by the rapid worldwide spread of the Argentine ant and the fire ant from their origin in South America [1,2]. On the other hand, the particular biology of ants, characterized by reproductive division of labor between highly fecund queens and sterile workers, allows the establishment of large populations from just one founding propagule. Introduced populations thus go through a genetic bottleneck, reducing diversity within the population while at the same time increasing diversity between populations [3]. Such populations then evolve in allopatry, and differences caused by genetic drift may be further amplified over time by selection, eventually leading to reproductive isolation. Reproductive isolation, in turn, together with the evolution of mating systems, underlies the formation of new species and, hence, the vast diversity of life. By allowing ants (and other organisms) to establish allopatric populations around the world, humans have inadvertently created a valuable scenario for studying species evolution in real time.

Reproductive isolation between populations that live in allopatry can evolve in the form of post-mating mechanisms of reproductive isolation (PoMRI). Importantly, PoMRI can result from Bateson–Dobzhansky–Muller (BDM) incompatibilities, in which two parental loci that have diverged cause hybrid sterility or inviability. Extending such negative epistatic interactions to the host's microbiome adds three mechanisms that can reduce hybrid fitness: hybrid susceptibility (i.e. inferior immune systems and higher pathogen loads in hybrids), hybrid autoimmunity (i.e. upregulation of immune functions in hybrids because of negative epistasis), and cytoplasmic incompatibility (CI, i.e. hybrid embryo death caused by incompatibilities between members of the parental microbiomes) [4]. PoMRI mechanisms can operate at any developmental stage and can directly affect the fitness of both hybrid offspring and mated parental females. The best-known cases of PoMRI caused by bacteria involve *Wolbachia*, the enigmatic evolutionary omnia rotundiora comprising endosymbionts and endoparasites [5], which infects at least 20% of the world's insect species, with estimates reaching up to 66% [6]. *Wolbachia* is famous for manipulating maternal transmission routes, most likely driven by an ancestral genomic association with a prophage [7]. *Wolbachia* strains capable of reproductive manipulation can sweep through

a population by inducing CI, or by favoring vertical maternal transmission via interference with the host's development, resulting in parthenogenesis, feminization, or male death [8].

Although numerous ant species are highly invasive and form allopatric populations on a global scale, nothing is known about PoMRI mechanisms involving endosymbiotic bacteria in these ecologically dominant insects. In particular, the functional role of *Wolbachia* in ant biology has thus far remained elusive, in spite of its omnipresence [9]. The globally distributed tramp ant *Cardiocondyla obscurior* has spread from its putative origin in Southeast Asia and today occurs in fruit tree plantations, city parks and other disturbed habitats in the tropics and sub tropics. In addition to *Wolbachia* populations of *C. obscurior* carry a main bacterial endosymbiont, *Cand.* Westeberhardia, which exhibits characteristics of an obligate symbiont (Klein et al. 2015). Populations of *C. obscurior* from Brazil (BR) and Japan (JP) show remarkable genomic heterogeneity and differ in a number of phenotypic traits [10]; nevertheless, mating between queens and males from the two populations readily takes place in the laboratory. However, a phenotype indicative of PoMRI was found in hybrid crosses between BR and JP populations, with BR queens mated to JP males exhibiting shorter lifespans and lower fecundity than BR queens mated to BR males [11]. At the time, this was attributed to BDM incompatibility of fast evolving sexual traits such as seminal fluid proteins, as suggested by an up-regulation of genes involved with immune response in outbred BR queens [11].

Here, we show that the negative effect on queen fitness is in fact caused by incompatible strains of *Wolbachia* harbored by the two populations. By reducing *Wolbachia* levels in males using antibiotic treatment, we demonstrate that queen fecundity can be rescued. Genomic analyses of the *Wolbachia* strains isolated from the two populations reveal that both strains belong to *Wolbachia* supergroup A, which typically contains strains capable of reproductive manipulation. Surprisingly, CI is only induced by the putatively ancestral strain, and this may be linked to functional differences in CI-associated loci. By discovering the first case of CI between two ant populations, our study provides the first description of functional *Wolbachia* infection dynamics in ants and presents a novel perspective on the biology of globally distributed ants.

Results

Unidirectional hybrid incompatibility

We verified the results from [11] by crossing queens and males from laboratory colonies of BR and JP populations collected in 2009 and 2010, respectively [10]. We conducted this experiment once in 2015 with the same outcome (Figure S1, Supplement Methods) and again in 2017/18, the results of which are presented here. As expected, compared to all other crosses the combination BR x JP (queen x male) resulted in lower fecundity as estimated by mean weekly egg number over the first six weeks after initiation of egg laying, regardless of whether the male was infected with *Cand.* Westeberhardia or not (Figure 1, Kruskal Wallis rank sum test, X^2= 78.04, df=6, p<0.001, see Table S1 for Bonferroni-Holm corrected pairwise p-values). Similar results were obtained when maximum weekly egg numbers were compared (Figure S2, Table S2, Kruskal Wallis rank sum test, X^2=81.10, df=6, p<0.001). Strikingly, the effect was even stronger when using males naturally uninfected with *Cand.* Westeberhardia, ruling out the possibility that this endosymbiont plays a role in the induction of reproductive isolation.

We monitored a subset of inter-population crosses for an additional 6 weeks (12 weeks in total). Of the 28 BR x JP colonies that were monitored for 12 weeks, seven failed to produce diploid offspring (queen/worker pupae), and four produced no pupae at all. We dissected the spermathecae of three of the seven male-only producing queens, and all contained sperm. All of the JP x BR colonies that were monitored for 12 weeks produced pupae, and they produced significantly more pupae than BR x JP (Figure 2A; Kruskal-Wallis rank sum test, X^2=27.90, df=2, Bonferroni-Holm corrected p<0.001). Furthermore, sex ratios of produced pupae were significantly more male-biased in BR x JP colonies compared to JP x BR colonies (Figure 2B; binomial GLM: $T_{2,52}$=32.81, Bonferroni-Holm corrected p<0.001), an effect caused entirely by the lack of developing females (Figure S3; Kruskal Wallis rank sum test, X^2=4.04, df=2, p=0.13). Together, these data show consistent incompatibility between BR queens and JP males.

Cytoplasmic incompatibility

Cytoplasmic incompatibility (CI) occurs when an endosymbiont favors its transmission by making infected males incompatible with uninfected females, while infected females can mate with both infected and uninfected males. A necessary test to verify CI is 'curing' the host of the putative CI-causing bacteria using antibiotic treatment, which should result in the 'rescue' of the wild-type phenotype.

We fed JP^{rif+} colonies the antibiotic rifampicin diluted in honey every other week for 10 weeks, which resulted in the complete loss of the main endosymbiont *Cand.* Westeberhardia (Figure S4; Mann-Whitney-U-Test, W=34, df=1, p<0.001) and a significant reduction of *Wolbachia* levels in workers (Figure S4; Mann-Whitney-U-Test, W=95, df=1, p<0.01). Treating colonies with the antibiotic tetracycline did not have a negative effect on *Wolbachia* (Figure S5; Mann-Whitney-U-Test, X^2=24, df=1, p=0.052). While *Cand.* Westeberhardia is permanently eradicated in subsequent generations the negative effect of rifampicin on *Wolbachia* is transient, with levels returning to normal 6 months after termination of treatment (Figure S6; *Cand.* Westeberhardia: Mann-Whitney-U-Test, W=64, df=1, p<0.001; *Wolbachia*: Mann-Whitney-U-Test, W=45, df=1, p=0.19). Five of 28 rifampicin-treated colonies succumbed to the treatment and died during the 10-week period, while all 28 control colonies survived.

Mating JP^{rif+} males collected shortly after ceasing antibiotic feeding with BR queens resulted in significantly rescued fecundity, although mean and maximum weekly egg numbers did not quite reach levels of BR and JP inbred queens (Figure 1, Table S1). This rescue effect was evident regardless of whether JP^{rif+} males came from *Cand.* Westeberhardia infected or uninfected colonies. Rescued BR x JP^{rif+} colonies also produced significantly more pupae over a 12-week period than their non-rescued BR x JP counterparts (Figure 2A; Kruskal-Wallis rank sum test, X^2=27.90, df=2, Bonferroni-Holm corrected p=0.027), and sex ratios among pupae were as female-biased as in JP x BR crosses (Figure 2B; binomial GLM: $T_{2,52}$=32.81, Bonferroni-Holm corrected p=0.011). Strongly reduced *Wolbachia* levels in JP^{rif+} males (Figure 3, Mann-Whitney-U-Test, W=163, df=1, p<0.001) support the role of *Wolbachia* in inducing hybrid incompatibility.

We confirmed unidirectional CI with males from laboratory colonies of a second Asian population collected in Taiwan (TW), which is infected with a *Wolbachia* strain that amplifies a *wsp* sequence (coding for the hypervariable *Wolbachia surface protein*) identical to those from JP samples (Figure S7). We set up crosses with queens from BR (BR x TW) and JP (JP x TW), and the reciprocal combination (TW x JP). Again, only the combination BR x TW resulted in reduced fecundity, both when mean weekly egg numbers (Figure S8; Kruskal Wallis rank sum test, X^2=9.96, df=2, p<0.01, see Table S3 for Bonferroni-Holm corrected pairwise p-values) and maximum weekly egg numbers over six weeks (Figure S8; Kruskal Wallis rank sum test, X^2=10.19, df=2, p<0.01, see Table S4 for Bonferroni-Holm corrected pairwise p-values) were compared.

Wolbachia genomics and phylogeny

We assembled the *Wolbachia* genomes from BR (*w*Cobs-BR) and JP (*w*Cobs-JP) populations of *C. obscurior* using Illumina HiSeq2000 100-bp reads of 200 and 500-bp insert paired-end libraries [10]. The genomes of both *Wolbachia* were assembled to 148 (BR) and 182 (JP) scaffolds (Table 1). Both strains showed similar genome sizes and G+C contents, with an estimated 1,013 (BR) and 1,058 (JP) predicted protein-coding genes. An analysis on shared genes revealed that both strains share a core of 907 proteins, with 85 unique to *w*Cobs-BR and 109 unique to *w*Cobs-JP. According to Bayesian phylogenetic analyses, both *Wolbachia* strains belong to supergroup A, which together with supergroup B contains strains capable of reproductive manipulation. *w*Cobs-JP was found to be more closely related to *w*Ha and *w*CauA strains, while *w*Cobs-BR was phylogenetically closer to *w*Au and *w*Mel (Figure 4A). A synteny analysis revealed that both *w*Cobs-JP and *w*Cobs-BR strains keep general synteny, but with several rearrangements (Figure 4B). This is consistent with previous observations of group A *Wolbachia* strains [12].

Wolbachia phenology

To compare infection titers between populations we performed qPCR of the *Wolbachia* gene *Cytochrome c oxidase subunit 1* (*coxA*) against the ant housekeeping gene *elongation factor 1-alpha 1* (*EF1*). JP queens had higher relative *w*Cobs-JP titers than BR queens infected with *w*Cobs-BR (Figure S9, Mann-Whitney-U-Test, W=23, df=1, p=0.043). Likewise, JP workers showed higher infection titers with *w*Cobs–JP compared to BR workers infected with *w*Cobs-BR (Figure S9, Mann-Whitney-U-Test, W=16, df=1, p=0.017).

To test for morph-bias in infection we compared *coxA* expression in adult queens, workers, winged males and wingless males using qPCR. *coxA* levels did not differ between sexes and were consistently higher in winged morphs (queens, winged males) compared to wingless morphs (workers, wingless males) (Figure S10, Kruskal Wallis rank sum test, X^2=19.53, df=3, p<0.001).

To measure the potential cost of *Wolbachia* infection and to test for a selective loss in workers, we compared infection levels of workers and queens over time. In contrast to *Cand.* Westeberhardia [13], *Wolbachia* levels quickly reached a plateau in both queens and workers. There was no indication that individuals lose *Wolbachia* over the first few weeks of their lives, which typically last for up to three (workers) or six months (queens) (Figure S11, workers: ANOVA, $F_{4,26}$= 2.69, p=0.059; queens: ANOVA, $F_{5,50}$= 15.95, p<0.001).

CI mechanism

CI usually results in the failure to produce viable zygotes but how CI operates functionally is still not clear. The two championed models are based on 1) a sperm modification step during spermatogenesis which is reversed by a rescue factor or 2) the transfer of a toxic product via the sperm and subsequent binding to a female-derived antidote [14]. The current genetic view for CI in *Drosophila* favors a two-by-one model [15], involving two adjacent genes (coined *cifA* and *cifB*) located in a region of prophage origin in *w*Mel [16], which contains several genes with eukaryote function [17]. Expression of both *cifA* and *cifB* in males is required to cause CI, while expression of *cifA* rescues embryo mortality in females [14].

We found orthologues of *cifA* and *cifB* in *Wolbachia* strains from BR and JP. In the latter, we found two additional paralogues. Through Bayesian phylogenetic inference, and following the classification scheme of [16], we found that all copies of *cifA* and *cifB* belong to their corresponding type. The *cifA* and *cifB* genes found in NODE_002 of *w*Cobs-JP are closely related to those found in *w*Cobs-BR and in the cryptic phage of strain *w*Sol isolated from the fig wasp *Ceratosolen solmsi* (Figure 5A, B). The *cifA* and *cifB* genes found in NODE_063 of *w*Cobs-JP show a more distant relationship to their homologues in *w*Cobs-BR. Following [16], we performed a protein remote homology search with the webserver of HHpred's v3.2.0 webserver [18]. While the *cifA* gene of *w*Cobs-BR contained a DUF249 domain, neither *cifA* homologues in *w*Cobs-JP showed homology to known domains (Figure 5C). In contrast, putative domains were found in all *cifB* genes. These shared a putative nuclease domain (PD-(D/E)XK nuclease/DpnII-MboI) found in other type I *cifB* genes. The *cifB* homologue found in NODE_063 in *w*Cobs-JP shared most domains with the *cifB* homologue in *w*Cobs-BR, with an additional peptidase domain (Peptidase_C58; PF03543).

Wolbachia in males

As mentioned above, *Wolbachia*-induced CI has often been linked to sperm modification during spermatogenesis [19] or the transfer of a CI toxin along with or in the sperm. The presence of *Wolbachia* in the testes is thus expected, although their specific localization in spermatocytes or spermatids might not be a prerequisite for inducing CI, as has been observed in the wasp *Nasonia vitripennis* [20]. We used fluorescence in situ hybridization to localize *Wolbachia* in the abdomens of male *C. obscurior*, confirming the presence of the bacteria throughout different tissues including the testes in both JP (Fig. 6A-C) and BR (Figure 6D) individuals. *Wolbachia* was also observed co-infecting bacteriocytes dominated by *Cand*. Westeberhardia, yet in significantly lower densities (Figure 6C).

Discussion

Insect-*Wolbachia* interactions can range from beneficial to detrimental and from facultative associations to rare cases of ultimate mutualisms where hosts have higher fitness with *Wolbachia* than without [5]. This prevalence and diversity of *Wolbachia* associations predictably also occurs in ants; however, our knowledge of ant-*Wolbachia* interactions is limited [9]. In the few ant-*Wolbachia* associations studied so far, infection is facultative (e.g. [21-23]), indicating ongoing arms races between hosts and symbionts [24]. One particularly obvious question to ask is whether *Wolbachia* has the power to control sex

allocation, a trait shaped by kin selection in social Hymenoptera [25]. In this context, facultative *Wolbachia* infections have been reported to cause transient changes in sex allocation (Pontieri et al. 2016), or to have no effect [22,26]. Similarly contrasting results have been obtained regarding effects on colony productivity [22,27]. It has furthermore been speculated that *Wolbachia* can bias caste ratios towards the production of queens [21,28], but current data are scarce and provide little support for this hypothesis [9]. By providing the first functional description of an ant-*Wolbachia* association involving two strains of *Wolbachia*, our study lays the groundwork for in-depth investigations into how *Wolbachia* affect ant reproductive biology and fitness.

Wolbachia clearly play a significant role in the biology of *C. obscurior*. First, all screened individuals were infected regardless of population, caste or sex. *Wolbachia* titers were higher in queens and winged males compared to workers and wingless males, a difference that is likely associated with the relative amounts of reproductive tissue as *C. obscurior* workers lack ovaries and winged males have larger testes than wingless males [29]. Second, rifampicin treatment merely reduced *Wolbachia* titers, and this effect was reversible. This was not the case for *Cand.* Westeberhardia, which was permanently cleared by rifampicin treatment. Third, *Wolbachia* titers did not decline with age in workers. *Wolbachia* infection can be costly and selection may thus favor reduced infection loads in sterile workers, as these do not contribute to vertical transmission [21,28]. Such a mechanism appears to be acting on *Cand.* Westeberhardia, where titers in workers (but not queens) decreased significantly with age, indicating that while the host may benefit from infection during development or in the adult egg-laying queen stage, the symbiont is not required [13]. Consistently high titers in workers indicate that *Wolbachia* do not have deleterious effects on worker performance in *C. obscurior*, unlike *Wolbachia* in *Acromyrmex* ants [30]. To what degree the population-specific strains differ in their effect on host phenotype remains unclear. Higher *Wolbachia* titers in JP individuals suggest that the *w*Cobs-JP strain may be better integrated into the host's biology. Alternatively, these differences may be driven by population-specific competition with *Cand.* Westeberhardia over limited resources.

Sex allocation in *C. obscurior* is female-biased [31] and queens presumably have full control over male production, as investment into males increases in the presence of competing queens [32-34], Accordingly, we found no indication that *Wolbachia* influences sex allocation. Queens from non-CI (JP x BR) crosses produced few males in the first 12 weeks of their lives. This may be a consequence of the short observation period, equaling ~50% of the average queen lifespan [31]. The sex ratios produced by CI (BR x JP) crosses showed a bimodal distribution, with several queens matching sex ratios produced by non-CI queens (albeit with lower overall productivity), while others produced only males. On average, however, CI queens did not produce more males than non-CI queens. There was also no indication that *Wolbachia* altered caste ratios towards production of queens. Concordantly, a previous study comparing investment into sexuals and workers did not find differences between the BR and JP populations [31]. Testing directly for a caste-biasing effect of *Wolbachia* requires complete elimination of the bacterium. While this cannot be done without also killing the ant host, preliminary trials indicate that cross-infection of the two *Wolbachia* strains is possible. In the future, such manipulations may help clarify whether *Wolbachia* have caste-manipulating power in *C. obscurior*.

329
330 Global exchange of stowaway ants leading to secondary contact between allopatric
331 populations is common (e.g. in the tropical fire ant *Solenopsis geminata* [35], and the little
332 fire ant *Wasmannia auropunctata* [36]) and thus the presented scenario, albeit conceived in
333 the laboratory, is not an unrealistic one. A previous study emphasized the role of BDM
334 incompatibility between allopatric *C. obscurior* populations in causing a CI-like phenotype
335 [11]. *Wolbachia*-induced incompatibilities were ruled out because of identity of a partial
336 sequence of *wsp* extracted from seven individuals (three from BR colonies collected in
337 2004, four from JP colonies collected in 2005) using the wsp81F/wsp691R primer
338 combination [37]. Gene expression analyses of allopatrically and sympatrically mated BR
339 queens pointed towards elevated immune responses and other changes that mimicked a
340 CI-like phenotype. In *Drosophila*, *Wolbachia* can manipulate expression of key regulatory
341 genes during spermatogenesis, which leads to embryonic lethality and a CI-like
342 phenotype [38]. Thus, what appeared to be BDM incompatibility may have been caused by
343 *Wolbachia* inducing a CI-like phenotype via interference with queen gene expression. The
344 alternative and more parsimonious explanation for the CI-like phenotype based on the
345 results from the present study is a classic unidirectional *Wolbachia*-driven CI effect
346 involving incompatible *Wolbachia* strains. This also explains why JP x BR crosses did not
347 elicit a CI phenotype. The overexpression of immunity-related genes in allopatrically
348 mated BR queens detected by Schrempf et al. 2015 may simply reflect physiological
349 responses to aborted oogenesis, as opposed to responses to ejaculate quality, or to
350 injuries caused by non-matching male genitalia. Furthermore, we recently found that some
351 BR colonies were infected with an additional *Wolbachia* strain displaying partial *wsp*
352 sequences identical to those of *w*Cobs-JP (data not shown), indicating horizontal
353 transfection in our rearing facilities, especially in older laboratory colonies.
354
355 The mechanism of CI in *C. obscurior* appears to align along the *Wolbachia cif*-like gene
356 axis described in *Drosophila* and *Culex* [15,16,39-41]. This genetic region, which is of prophage
357 origin and capable of manipulating the eukaryote host, showcases the importance of
358 using a hologenomic approach to study evolution [42]. *w*Pip of *Culex pipiens* and *w*Yak of *D.*
359 *yakuba* have similar prophage-derived regions containing two syntenic pairs of paralog
360 genes (termed *cidA*/*cidB* and *cinA*/*cinB)* [43]. *cidA*/*cidB* have been suggested to induce and
361 rescue CI via a toxin-antidote mechanism where *cidB* acts as a modifier and *cidA* as a
362 rescuer [41]. Surprisingly, the paralog genes *cidA*/*cifA* in *w*Pip and *w*Mel have different
363 biochemical functions: both contain ankyrin-like repeats for protein-protein interaction
364 with eukaryotic DNA [41] but *cifA* is not a putative deubiquitinase [14], as postulated for *cidA*
365 [39]. Both *Wolbachia* strains isolated from *C. obscurior* have orthologues of *cifA* and *cifB* but
366 only the *w*Cobs-JP strain has an additional *cifA*/*B*-like pair, pointing towards a role for the
367 latter pair in inducing reproductive isolation. Whether the second *cifA*/*B* containing region
368 was lost in *w*Cobs-BR, or whether it stems from a duplication event and subsequent
369 divergence in *w*Cobs-JP as has been described for the *w*AlbB strain of *Aedes albopictus*
370 [44], remains to be shown. Alternatively, functional differences in *cifA*/*B* orthologues
371 between *w*Cobs-JP and *w*Cobs-BR, or an interaction of the two *cif*-like gene products in JP
372 males could be causing the CI. Irrespective of the exact CI mechanism, it remains unclear
373 why a mere reduction of *Wolbachia* titers in males was sufficient to rescue queen
374 fecundity. This requires studying the effects of *Wolbachia* on sperm production. One
375 possibility is that rifampicin treatment causes ribosomal stress that prevents *Wolbachia*

from modifying sperm. We also do not know why the CI effect was stronger when using males from colonies naturally uninfected with *Cand*. Westeberhardia, but this points towards interaction effects between the two symbionts.

Our study raises many questions about the evolutionary history of the *C. obscurior-Wolbachia* association. The putative origin of *C. obscurior* in Southeast Asia, together with sequence identity between *Wolbachia* strains found in Japan and Taiwan, suggest that these strains represent the more ancestral association. Geographic patterning separating New from Old World *Wolbachia* strains has been observed previously in ants [45], and frequent horizontal transmissions [46,47] can lead to a surprising diversity within species [48]. *C. obscurior* and its sister species *C. wroughtonii* are the only known representatives of the 100+ described species in the genus *Cardiocondyla* (the so-called heart-node ants) that have adopted an arboreal lifestyle, as opposed to nesting in soil and rock crevices. This makes them highly susceptible to horizontal transmission of *Wolbachia* from other plant-associated insects. How exactly the BR population acquired a novel strain of *Wolbachia* in the New World habitat, and how this strain subsequently replaced the ancestral strain, is unclear, however. Although *Wolbachia* from different supergroups may co-exist in a host [12], it is unlikely that two strains from the same supergroup co-exist without eventually recombining and merging. Generally, unidirectional CI should facilitate introgression between populations, while bidirectional CI should promote divergence. This predicts mixed *C. obscurior* genotypes but only the presence of the *w*Cobs-JP strain in secondary contact zones, assuming that hybrids perform as well as parental lineages. But how has the ancestral Asian strain be replaced? *Wolbachia* acquisition and persistence in *C. obscurior* may be driven by selection on the strain that is better adapted to the local environment, perhaps analogous to *Wolbachia*-driven thermal preferences in *Drosophila* flies [49,50]. Resolving how *w*Cobs-BR replaced the putatively ancestral *w*Cobs-JP strain (which holds the power of CI) requires testing how mixed combinations of host and *Wolbachia* perform under varying ecological conditions. Coupled with a global survey of *Wolbachia-C. obscurior* associations, this will help unravel how the symbiosis shapes the worldwide distribution of this tramp ant.

Conclusion

One important consequence of unidirectional reproductive isolation is unequal inheritance, which allows a BDM-causing locus or a reproductive manipulator to quickly spread in secondary contact zones. Such disruptive factors can be more powerful than natural selection on other fitness-relevant traits, and lead to the evolution of PoMRI and hybrid inviability, processes estimated to require several million years in *Drosophila* flies and *Pogonomyrmex* ants [51,52]. Our discovery of reproductive isolation between allopatric ant populations, driven by two naturally occurring, closely related *Wolbachia* strains that differ in their genomic makeup, demonstrates that these evolutionary processes can be observed in real time and lays the groundwork for detailed studies of *Wolbachia*-ant biology. In particular, a system in which CI is accompanied by a CI-like phenotype in host gene expression may prove useful for understanding the function of the *cid/cin* gene family. Hopefully, hologenomic approaches such as the one presented here will help provide the comprehensive understanding of species' biology needed to tackle the challenges associated with human-induced changes to ecological and evolutionary dynamics.

423
424 Methods
425 *Cardiocondyla obscurior* presumably originates from Southeast Asia and is now
426 distributed around the tropics and subtropics. Queens in *C. obscurior* are produced year-
427 round and have a short generation time of ~120 days (from egg to queen to egg).
428 Colonies usually contain 2-5 queens [10] and a single wingless male that can live up to a few
429 months and continually produces sperm [53]. Such males transfer on average 1000 sperm
430 cells per copulation [54], which is sufficient for a lifelong production of diploid offspring by
431 an inseminated queen. Newly hatched queens can decide to stay in the maternal nest or
432 to leave - alone or with a small group of workers - irrespective of mating status. Like all
433 Hymenoptera, ants exhibit haplodiploid sex determination and virgin females can
434 produce males from haploid, unfertilized eggs. Virgin queens in *C. obscurior* can copulate
435 with their own sons (pers. obs.), enabling the production of workers and queens, similar to
436 a related *Cardiocondyla* species [55]. This biology has facilitated the worldwide spread of
437 several species of the genus [56].
438
439 In this study, we used inbred laboratory 'populations' derived from colonies collected in
440 Okinawa, Japan in 2010 (JP) and Bahia, Brazil in 2009 (BR). Although the two populations
441 differ in cuticular hydrocarbon composition, queen size and behavior [10], workers are
442 morphologically indiscernible according to exploratory data analyses by hierarchical and
443 nonhierarcical, vector-based forms of Nest Centroid clustering: NC-Ward, NC-part.hclust,
444 NC-part.kmeans, NC-NMDS-kmeans [57,58]. These analyses considered 15 continuous
445 morphometric characters. Specifically, when considering 82 cosmopolitan nest samples of
446 the sister taxa *C. wroughtonii* and *C. obscurior*, all JP and BR samples were allocated to the
447 latter species by all four types of NC-clustering. This result was confirmed with posterior
448 probabilities of $p > 0.98$ if these samples were run as wild-cards in a linear discriminant
449 analysis. Analyses of 32 nest samples representing only the *C. obscurior* cluster could not
450 allocate the JP and BR populations to different intraspecific clusters nor could these
451 analyses demonstrate any intraspecific structuring at all. This suggests that *Wolbachia*-
452 induced reproductive isolation has not yet led to a divergence into morphospecies. In
453 addition to JP and BR colonies, we used colonies collected from a second Asian
454 population in Taipei, Taiwan in 2013 (TW) to confirm the presence of unidirectional CI. For
455 all experiments, colonies were kept in square plaster-bottom nests (100 x 100 x 20 mm,
456 Sarstedt, Germany) and held in climate chambers under a 12h/12h light/dark cycle and a
457 28°C/22°C temperature cycle. Food (honey and *Drosophila* or pieces of *Periplaneta*
458 *americana*) and water were provided to stock colonies every 3 days. All animal treatment
459 guidelines applicable to ants under international and German law were followed.
460 Collection of colonies that form the basis of the laboratory population used in this study
461 was permitted by the Brazilian Ministry of Science and Technology (RMX 004/02). No other
462 permits were required for this study.
463
464 Antibiotic treatment
465 Rifampicin is a broad-spectrum antibiotic that acts via inhibition of bacterial RNA
466 polymerase [59]. To produce *Wolbachia*-cured males, we split large *Cand*. Westeberhardia-
467 infected (JP) and uninfected (JP_{we-}) stock colonies into two equal halves. Half of these splits
468 were designated as controls (JP: n=13, JP_{we-}-: n=5), while the other half was treated with
469 antibiotics (JP: n=13, JP_{we-}: n=5). We diluted 0.0025 g of solid rifampicin (Sigma-Aldrich,

470 USA) in 500 µl of a 1:1 honey-water solution for a final antibiotic concentration of 0.5%.
471 The antibiotic solution was placed on a shaker for 4 hours to ensure complete mixing, and
472 subsequently covered with aluminum foil and stored at -20°C. Treated colonies were fed
473 with the antibiotic solution twice per week every other week, for a total duration of ten
474 weeks. On the days following treatment, the antibiotic solution was removed from the
475 nest. Between antibiotic feedings (i.e. every other week), colonies were fed with honey
476 and pieces of autoclaved cockroach (to prevent bacterial re-infections) and water ad
477 libitum. Control colonies were fed twice a week with honey and cockroaches and received
478 water ad libitum.
479
480 ***Wolbachia* and *Cand.* Westeberhardia infection**
481 We assessed the presence and titers of bacterial infections using PCR and qPCR,
482 respectively, on DNA extracted from whole bodies (worker pupae & adults, queen pupae
483 & adults, adult males). DNA was extracted from samples using a standard CTAB protocol.
484
485 *Presence of infection*
486 We confirmed infection in a subset of workers from BR and JP colonies. Infection with
487 *Wolbachia* was tested with a PCR assay using primers specific for a fragment of the
488 *Wolbachia surface protein* gene of the BR (105-bp, *wsp_wCobs_BR-for: 5-*
489 *'TAAATCTTGCATCTGTAACATT-3',* *wsp_wCobs_BR-rev: 5'-*
490 *CTGCGGATACTGATACAACTACTG-3'*) and JP (254-bp, *wsp_wCobs_JP-for: 5'-*
491 *CATTTTGACTACTCACAGCGGTTG-3',* *wsp_wCobs_JP-rev:*
492 *5'CTGCGGATACTGATACAACTACTG-3'*) strains. *Cand.* Westeberhardia infection was
493 tested by amplifying a 204-bp fragment of the *ribonucleoside-diphosphate reductase 1*
494 *subunit beta* gene of *Westeberhardia* (*WEOB_403*) (*nrdB_weCobs-for:* 5'-
495 GGAAGGAGTCCTAATGTTGCG-3'; nrdB_*weCobs*-rev: 5'-ACC
496 AGAAATATCTTTTGCACGTT-3'). A 104-bp fragment of the *C. obscurior* gene *elongation*
497 *factor 1-alpha 1* (*Cobs_01649*) (*EF1-for:* 5'-TCACTGGTACCTCGCAAGCCGA-3'; *EF1-rev:*
498 5'-AGCGTGCTCACGAGTTTGTCCG-3') was used as a positive control. In addition,
499 infection was assessed in two adult queens from each of five TW colonies to confirm that
500 this population carries the *w*Cobs-JP strain. Each PCR reaction contained 5 µL Taq
501 polymerase (GoTaq, Promega), 3 µL H_2O, 0.5 µL forward primer (10 µM), 0.5 µL reverse
502 primer (10 µM) and 1 µL DNA. PCRs were run at 94°C for 4 minutes followed by 36 cycles
503 at 94°C for 30s, 57°C for 30s and 72° for 30s, with a final step of 72°C for 10 minutes.
504 Electrophoresis separation of PCR products was performed on a 1.5% TAE-Gel with 0.5 µl
505 of 0.001 % Gel-Red for 45 minutes at 60 V and 65 mA.
506
507 *Population-specific Wolbachia titers*
508 We compared *Wolbachia* infection titers of adult workers and queens from BR (n=9
509 workers, n=10 queens) and JP (n=10 workers, n=9 queens) colonies by amplifying a
510 portion of the *Cytochrome c oxidase subunit 1* gene (*coxA_wCobs-for*: 5'-
511 TTGGTCATCCAGAAGTTTACGT-3', *coxA_wCobs-rev*: 5'-TGAGCCCAAACCATAAAGCC-
512 3') in qPCR. As a relative standard *elongation factor 1-alpha 1* (*Cobs_01649*) was used.
513 Each qPCR reaction contained 5 µL SYBR (Peqlab), 2 µL H_2O, 1 µL forward primer (2 µM), 1
514 µL reverse primer (2 µM) and 1 µL DNA. Reactions were performed in duplicates and run
515 at 95°C for 3 minutes followed by 40 cycles at 95°C for 5s, 60°C for 20s, and 95° for 10s,
516 and a final melt curve analysis step in which reactions were heated from 65°C to 95°C in

517 5°C steps. Single-amplicon production was confirmed with melt curve analyses and
518 relative *Wolbachia* titers calculated with the $2^{-\Delta CT}$ method [60].
519
520 *Age and morph-specific Wolbachia titers*
521 We quantified *Wolbachia* titers in individual queens and workers from BR colonies by
522 determining relative *coxA_wCobs* copy numbers with qPCR across developmental stages
523 and adult age classes. In workers, titers were measured in pupae (n=4 white pupae, n=5
524 dark pupae) and in adults two days (n=5), 14 days (n=7), and 28 days (n=6) post-hatching.
525 In queens, titers were measured in pupae (n=5 white pupae, n=4 dark pupae), as well as in
526 adults two days (n=7), 14 days (n=7), 28 days (n=10 virgin queens, n=7 mated queens)
527 and 48 days (n=9) post-hatching. In addition, we quantified *coxA_wCobs* copy numbers in
528 adult morphs (n=15 queens, n=12 workers, n=6 winged males, n=7 wingless males). For
529 all reactions, *elongation factor 1-alpha 1* (*Cobs_01649*) was used as a housekeeper. Each
530 qPCR reaction contained 5 µL SYBR (Peqlab), 2 µL H_2O, 1 µL forward primer (2 µM), 1 µL
531 reverse primer (2 µM) and 1 µL DNA. Reactions were performed in triplicates and run as
532 described above. Single-amplicon production was confirmed with melt curve analyses and
533 relative quantities of *Wolbachia* calculated with the $2^{-\Delta CT}$ method.
534
535 *Rifampicin effects on infection titers*
536 We verified the efficacy of rifampicin treatment by measuring *Wolbachia* and
537 *Westeberhardia* titers in dark worker pupae produced by antibiotic-treated (n=21 from 9
538 colonies) and control colonies (n=21 from 8 colonies) using qPCR of *coxA_wCobs and*
539 *nrdB_weCobs*. In addition, we measured the *Wolbachia* titers of JP males used in mating
540 combinations BR x JP and BR x JP^{rif+} (JP: n=15, JP^{rif+}: n=12) with qPCR of a portion of the
541 JP-specific *wsp* gene (*wsp_wCobs_JP*). For all samples, *elongation factor 1-alpha 1*
542 (*Cobs_01649*) was used as a housekeeper. Each qPCR reaction contained 5 µL SYBR
543 (Peqlab), 2 µL H_2O, 1 µL forward primer (2 µM), 1 µL reverse primer (2 µM) and 1 µL DNA.
544 Reactions were performed in duplicates (males) or triplicates (worker pupae) and run as
545 described above (except with an annealing temperature of 57°C for male pupae). Single-
546 amplicon production was confirmed with melt curve analyses and relative quantities of
547 *Wolbachia* and *Westeberhardia* calculated with the $2^{-\Delta CT}$ method.
548
549 Experimental crosses
550 We designed seven mating combinations between queens and males from the two
551 populations: 1) JP x JP (n=7), 2) JP x BR (n=26), 3) BR x BR (n=11), 4) BR x JP (n=36), 5) BR
552 x JP_{we-} (n=29), 6) BR x JP^{rif+} (n=13) and 7) BR x JP_{we-}^{rif+} (n=5). Each experimental colony was
553 set up with one dark queen pupa, one freshly hatched male, 10 workers and brood (10
554 eggs, 10 larvae, 10 worker pupae). All individuals were collected from un-manipulated
555 stock colonies, except for JP^{rif+} and JP_{we-}^{rif+} males used in combinations #6 and #7, which
556 were collected from rifampicin-treated colonies. To avoid manipulation effects, all
557 combinations were set up in parallel. In such experimental colonies, mating between
558 queens and males usually occurs within three weeks, after which queens shed their wings
559 and being laying eggs. We monitored colonies for queen wing loss once per week. Once
560 queens had shed their wings, we removed any brood placed in the colony during set up
561 and standardized worker number to 20. Colonies were then monitored once a week for six
562 weeks and all eggs and pupae (queen, worker, wingless male, winged male) counted. A
563 subset of colonies was monitored for a total of 12 weeks (JP x BR: n=19, BR x JP: n=28, BR

564 x JP^{rif+}: n=9). In each colony, the number of adult workers was kept constant at 20
565 individuals by removing hatched workers or adding workers from stock colonies. From
566 monitoring data, we calculated mean and maximum weekly egg numbers, and total
567 number and sex ratio of produced pupae (male pupae:total pupae).
568
569 To verify that CI is specifically induced by the *w*Cobs-JP strain when it encounters the
570 *w*Cobs-BR strain, we set up three additional mating combinations between queens and
571 males using a third population from Taiwan (TW) which also harbors the *w*Cobs-JP strain:
572 1) JP x TW (n=5), 2) TW x JP (n=6), 3) BR x TW (n=5). Experimental colonies were set up
573 and monitored as described above for six weeks.
574
575 **DNA sequencing and genome assembly**
576 We extracted DNA from a pool of 26 (JP) and 30 (BR) males from two colonies, collected
577 in 2009 in Una, Brazil (BR2009-alpha) from aborted fruits of coconut trees and in 2010 in
578 Naha, Japan (JP2010-OypB) from under bark of coral trees (*Erythrina* sp.). For details see
579 [10]. Briefly, the reads were right-tail clipped (minimum quality of 20) and all reads with
580 undefined nucleotides were removed using a combination of FASTX-Toolkit v0.0.14
581 (http://hannonlab.cshl.edu/fastx_toolkit/, last accessed December 3, 2010) and
582 PRINSEQ++ v1.2 (10.7287/peerj.preprints.27553v1). The resulting paired end reads were
583 assembled with SPAdes v3.13.1 (-k 33,55,77 --only-assembler [61]. The resulting contigs
584 were then binned according to an *ad hoc* BLASTX-based method. First, a proteome
585 database was built from representative genomes (Table S5). Second, the best hit for each
586 scaffold was used for assigning a preliminary bin and a coverage cut-off (10x for BR and
587 30x for JP) was implemented based on the coverage of the longest contigs. Third, each
588 scaffold was manually inspected using the online NCBI web-server *vs.* BLAST+2.9.0. If the
589 best hits to proteins were consistently to *Wolbachia* bacteria across the scaffold, the query
590 sequence was retained. Finally, the assembly graph was loaded into Bandage v0.8.1 [62],
591 the graph(s) matching *Wolbachia* sequences were identified and the sequences were
592 extracted. These extracted sequences were then compared to the *Wolbachia* draft bin. In
593 both cases, the extracted sequences were roughly the same compounded length as the
594 manually-curated bins and added only a couple of kilo base pairs (kbp), suggesting near
595 completeness of the genome. Using these *Wolbachia* bins, we performed a mapping
596 using BOWTIE2 v2.3.4.1 [63] followed by a re-assembly of the mapped reads in SPAdes
597 (with previously-mentioned parameters). This final reassembly was filtered by both
598 coverage and manual screening of scaffolds shorter than 3 kbp. Assembled sequences
599 have been deposited in the European Nucleotide Archive (ENA) under the accessions
600 CACTIU010000000.1 (*w*Cobs-BR) and CACTIV010000000.1 (*w*Cobs-JP).
601
602 **Phylogeny and comparative genomics of *Wolbachia* strains**
603 A draft annotation of the scaffolds was done using Prokka v1.14 [64]. For comparative
604 genomic purposes, we built a subset of the predicted ORFs by filtering out all proteins
605 annotated as "hypothetical proteins" with genes shorter than 300 base pairs (bp). This
606 helped us avoid wrongly annotated ORFs overlapping pseudogenes. To infer the
607 phylogenetic relationship between *Wolbachia* strains found to infect the analysed BR and
608 JP populations as well as among other *Wolbachia* bacteria, we collected the amino acid
609 sequences for the ribosomal proteins of 23 *Wolbachia* strains from supergroups A (8), B
610 (10), C (2), D (1), E (1), and F (1) (Table S6). Using *Anaplasma phagocytophilum* strain HZ

611 and *Ehrlichia canis* strain Jake as outgroups, we inferred a Bayesian phylogeny using
612 MrBayes v3.2.6 [65]. We ran two independent analyses with four chains each for 300,000
613 generations and checked for convergence. The substitution model JTT+I+G+F was used
614 as suggested by jModelTest v2.1.10.
615
616 To infer the shared protein-coding gene content of *w*Cobs-BR and *w*Cobs-JP strains, we
617 used OrthoMCL v2.0.9 [66,67] with an inflation value of 1.5. The synteny of both strains was
618 assessed using nucmer v3.23 [68] using anchor matches that were unique in both the
619 reference and query (--mum).
620
621 **Cif-family gene annotation and phylogenetics**
622 *cif* genes were first identified by BLASTP using the protein sequences WP_010962721.1
623 (*cifA*) and WP_010962722.1 (*cifB*) as references. Predicted start codons were manually
624 checked for the presence of a Shine-Dalgarno-like sequence. To identify whether the *cif*
625 genes form each strain belonged to the same type or not, we performed a phylogenetic
626 analysis following Lindsey *et. al.* 2018. Briefly, the previously used protein sequences were
627 aligned with the newly acquired ones from both wCobs-BR and wCobs-JP. The alignments
628 were then back-translated to nucleotides. For *cifB*, the type IV genes were excluded and
629 the 3'-end of the alignment was manually truncated to remove the longer unmatched
630 regions of some *cifB* variants. Bayesian phylogenetic inference was performed with
631 MrBayes v3.2.6 with the GTR+G substitution model (as suggested by jModelTest) running
632 two independent analyses with four chains each for 1,000,000 generations, and checked
633 for convergence. Following [16], Cif protein domains were searched for using HHpred's
634 v3.2.0 webserver (https://toolkit.tuebingen.mpg.de/tools/hhpred) with default parameters
635 and the following databases: SCOPe70 v2.07, COG/KOG v1.0, Pfam-A v32.0, and SMART
636 v6.0. hits with a probability >=80% were considered.
637
638 All genomic data files are available at the zenodo repository
639 https://doi.org/10.5281/zenodo.3561160
640
641 **Histological sectioning and fluorescence in situ hybridization**
642 *C. obscurior* (JP) male abdomens were fixed in 4% formaldehyde in PBS and washed with
643 water followed by a dehydration series in n-Butanol (30%, 50%, 70%, 80%, 90%, 96%) at
644 room temperature with shaking for 1 h at each step. Absolute n-butanol was used for the
645 last three hours at 30°C, exchanging the solution each hour. Dehydrated samples were
646 embedded in Technovit 8100 cold polymerizing resin (Heraeus Kulzer, Germany)
647 according to the manufacturer's instructions, cut into semithin sections (8 µm) with a
648 Microm HM355S microtome (Thermo Fisher Scientific, Germany) and mounted on glass
649 slides coated with poly-L-lysine (Kindler, Germany). The tissue sections were incubated for
650 90 min at 50°C in hybridization buffer (0.9 M NaCl, 20 mM Tris/HCl (pH 8.0), 0.01 % SDS)
651 containing 0.5 µM of the *Wolbachia*-specific probes Wolb_W2_Cy5 (5'-
652 CTTCTGTGAGTACCGTCATTATC-3') [69] and Wolb_Wol3_Cy5 (5'-
653 TCCTCTATCCTCTTTCAATC-3'), [70], as well as the *Cand*. Westeberhardia-specific probe
654 Wcard1_Cy3 (5'- ATCAGTTTCGAACGCCATTC-3') [13]. DAPI (4',6-diamidino-2-
655 phenylindole) was used for host DNA counterstaining. After hybridization, samples were
656 washed with buffer (0.1 M NaCl, 20 mM Tris/HCl (pH 8.0), 5mM EDTA, 0.01% SDS) for 20
657 min at 50°C. Subsequently, the washing buffer was removed and washed with distilled

658 water for 20 min at 50°C. Samples were air-dried and covered with VectaShield® (Vector
659 Laboratories, Burlingame, CA, USA) and stored overnight at room temperature. Images
660 were acquired on an AxioImager.Z1 epifluorescence microscope (Carl Zeiss, Jena,
661 Germany).
662
663 Acknowledgements
664 The authors thank John Wang for help collecting colonies in Taiwan and for providing the
665 *wsp* sequence of the TW population. We thank Julia Hacker for help with the BR x TW
666 crossings and Helena Lowack and Jennifer Wallner for help with lab work. JD Shropshire
667 helped with the *cid/cif/cin* annotation and Benjamin Weiss assisted with histological
668 preparations. This work was supported by the Marie-Curie AgreenSkills+ fellowship
669 program cofunded by the EU's Seventh Framework Programme (FP7-609398) to A.M.M,
670 and a DFG grant He1623/31 to JH and JO.
671
672 References
673 1. Wetterer, J. K., Wild, A. L., Suarez, A. V., Roura-Pascual, N. & Espadaler, X.
674 Worldwide spread of the Argentine ant, *Linepithema humile* (Hymenoptera:
675 Formicidae). *Myrmecol News* **12,** 187–194 (2009).
676 2. Ascunce, M. S. *et al.* Global invasion history of the fire ant *Solenopsis invicta*. *Science*
677 **331,** 1066–1068 (2011).
678 3. Tsutsui, N. D., Suarez, A. V., Holway, D. A. & Case, T. J. Reduced genetic variation
679 and the success of an invasive species. *Proc Natl Acad Sci U S A* **97,** 5948–5953
680 (2000).
681 4. Brucker, R. M. & Bordenstein, S. R. Speciation by symbiosis. *Trends in Ecology &*
682 *Evolution* **27,** 443–451 (2012).
683 5. Zug, R. & Hammerstein, P. Bad guys turned nice? A critical assessment of *Wolbachia*
684 mutualisms in arthropod hosts. *Biological Reviews* **90,** 89–111 (2014).
685 6. Hilgenboecker, K., Hammerstein, P., Schlattmann, P., Telschow, A. & Werren, J. H.
686 How many species are infected with *Wolbachia*?--A statistical analysis of current
687 data. *FEMS Microbiology Letters* **281,** 215–220 (2008).
688 7. LePage, D. P. *et al.* Prophage WO genes recapitulate and enhance *Wolbachia*-
689 induced cytoplasmic incompatibility. *Nature* **543,** 243–247 (2017).
690 8. Werren, J. H. Biology of *Wolbachia*. *Annu. Rev. Entomol.* **42,** 587–609 (1997).
691 9. Russell, J. A. The ants (Hymenoptera: Formicidae) are unique and enigmatic hosts of
692 prevalent *Wolbachia* (Alphaproteobacteria) symbionts. *Myrmecol News* **16,** 7–23
693 (2012).
694 10. Schrader, L. *et al.* Transposable element islands facilitate adaptation to novel
695 environments in an invasive species. *Nature Communications* **5,** 5495 (2014).
696 11. Schrempf, A. *et al.* Mating with an allopatric male triggers immune response and
697 decreases longevity of ant queens. *Molecular Ecology* **24,** 3618–3627 (2015).
698 12. Ellegaard, K. M., Klasson, L., Näslund, K., Bourtzis, K. & Andersson, S. G. E.
699 Comparative genomics of *Wolbachia* and the bacterial species concept. *PLoS Genet*
700 **9,** e1003381 (2013).
701 13. Klein, A. *et al.* A novel intracellular mutualistic bacterium in the invasive ant
702 *Cardiocondyla obscurior*. *ISME J* **10,** 376–388 (2016).
703 14. Shropshire, J. D. & Bordenstein, S. R. Two-By-One model of cytoplasmic
704 incompatibility: Synthetic recapitulation by transgenic expression of cifA and cifB in

705 *Drosophila*. *PLoS Genet* **15,** e1008221 (2019).
706 15. Shropshire, J. D. *et al.* Models and Nomenclature for Cytoplasmic Incompatibility:
707 Caution over Premature Conclusions - A Response to Beckmann et al. *Trends Genet.*
708 **35,** 397–399 (2019).
709 16. Lindsey, A. R. I. *et al.* Evolutionary Genetics of Cytoplasmic Incompatibility Genes
710 cifA and cifB in Prophage WO of *Wolbachia*. *Genome Biology and Evolution* **10,**
711 434–451 (2018).
712 17. Perlmutter, J. I. *et al.* The phage gene wmk is a candidate for male killing by a
713 bacterial endosymbiont. *PLoS Pathog* **15,** e1007936 (2019).
714 18. Zimmermann, L. *et al.* A Completely Reimplemented MPI Bioinformatics Toolkit with
715 a New HHpred Server at its Core. *J. Mol. Biol.* **430,** 2237–2243 (2018).
716 19. Veneti, Z. *et al.* Cytoplasmic incompatibility and sperm cyst infection in different
717 *Drosophila-Wolbachia* associations. *Genetics* **164,** 545–552 (2003).
718 20. Clark, M. E. *et al. Wolbachia* modification of sperm does not always require
719 residence within developing sperm. *Heredity* **101,** 420–428 (2008).
720 21. Wenseleers, T., Sundstrom, L. & Billen, J. Deleterious *Wolbachia* in the ant *Formica*
721 *truncorum*. *Proceedings of the Royal Society B: Biological Sciences* **269,** 623–629
722 (2002).
723 22. Pontieri, L., Schmidt, A. M., Singh, R., Pedersen, J. S. & Linksvayer, T. A. Artificial
724 selection on ant female caste ratio uncovers a link between female-biased sex ratios
725 and infection by *Wolbachia* endosymbionts. *J Evolution Biol* **30,** 225–234 (2017).
726 23. Shoemaker, D. D., Ross, K. G., Keller, L., Vargo, E. L. & Werren, J. H. *Wolbachia*
727 infections in native and introduced populations of fire ants (*Solenopsis spp.*). *Insect*
728 *Molecular Biology* **9,** 661–673 (2000).
729 24. Correa, C. C. & Ballard, J. W. O. *Wolbachia* Associations with Insects: Winning or
730 Losing Against a Master Manipulator. *Front. Ecol. Evol.* **3,** 506 (2016).
731 25. Trivers, R. L. & Hare, H. Haploidploidy and the evolution of the social insect. *Science*
732 **191,** 249–263 (1976).
733 26. Keller, L. *et al.* Sex ratio and *Wolbachia* infection in the ant *Formica exsecta*. *Heredity*
734 **87,** 227–233 (2001).
735 27. Singh, R. & Linksvayer, T. A. The bacterial endosymbiont *Wolbachia* increases
736 reproductive investment and accelerates the life cycle of ant colonies. **90,** 89
737 28. Treanor, D., Pamminger, T. & Hughes, W. O. H. The evolution of caste-biasing
738 symbionts in the social hymenoptera. *Insect. Soc.* **65,** 513–519 (2018).
739 29. Schrempf, A., Moser, A., Delabie, J. & Heinze, J. Sperm traits differ between winged
740 and wingless males of the ant *Cardiocondyla obscurior*. *Integrative Zoology* **11,**
741 427–432 (2016).
742 30. Andersen, S. B., Boyle, M., Nash, D. R. & Boomsma, J. J. Dynamic *Wolbachia*
743 prevalence in *Acromyrmex* leaf-cutting ants: potential for a nutritional symbiosis. *J*
744 *Evolution Biol* **25,** 1340–1350 (2012).
745 31. Kramer, B. H., Schrempf, A., Scheuerlein, A. & Heinze, J. Ant Colonies Do Not Trade-
746 Off Reproduction against Maintenance. *PLoS ONE* **10,** e0137969 (2015).
747 32. Cremer, S. & Heinze, J. Adaptive production of fighter males: queens of the ant
748 *Cardiocondyla* adjust the sex ratio under local mate competition. *Proc. Biol. Sci.*
749 **269,** 417–422 (2002).
750 33. de Menten, L., Cremer, S., Heinze, J. & Aron, S. Primary sex ratio adjustment by ant
751 queens in response to local mate competition. *Animal Behaviour* **69,** 1031–1035

752 (2005).
753 34. Suefuji, M., Cremer, S., Oettler, J. & Heinze, J. Queen number influences the timing
754 of the sexual production in colonies of *Cardiocondyla* ants. *Biol. Lett.* **4,** 670–673
755 (2008).
756 35. Gotzek, D., Axen, H. J., Suarez, A. V., Helms Cahan, S. & Shoemaker, D. Global
757 invasion history of the tropical fire ant: a stowaway on the first global trade routes.
758 *Molecular Ecology* **24,** 374–388 (2015).
759 36. Foucaud, J. *et al.* Worldwide invasion by the little fire ant: routes of introduction and
760 eco-evolutionary pathways. *Evol Appl* **3,** 363–374 (2010).
761 37. Braig, H. R., Zhou, W., Dobson, S. L. & O'Neill, S. L. Cloning and characterization of a
762 gene encoding the major surface protein of the bacterial endosymbiont *Wolbachia*
763 pipientis. *Journal of Bacteriology* **180,** 2373–2378 (1998).
764 38. Clark, M. E., Heath, B. D., Anderson, C. L. & Karr, T. L. Induced paternal effects
765 mimic cytoplasmic incompatibility in *Drosophila*. *Genetics* **173,** 727–734 (2006).
766 39. Beckmann, J. F., Ronau, J. A. & Hochstrasser, M. A *Wolbachia* deubiquitylating
767 enzyme induces cytoplasmic incompatibility. *Nat Microbiol* **2,** 17007–7 (2017).
768 40. Beckmann, J. F. *et al.* The Toxin-Antidote Model of Cytoplasmic Incompatibility:
769 Genetics and Evolutionary Implications. *Trends Genet.* **35,** 175–185 (2019).
770 41. Bonneau, M. *et al. Culex pipiens* crossing type diversity is governed by an amplified
771 and polymorphic operon of *Wolbachia*. *Nature Communications* **9,** 319–10 (2018).
772 42. Brucker, R. M. & Bordenstein, S. R. The Hologenomic Basis of Speciation: Gut
773 Bacteria Cause Hybrid Lethality in the Genus *Nasonia*. *Science* (2013).
774 doi:10.1126/science.1240659
775 43. Cooper, B. S., Vanderpool, D., Conner, W. R., Matute, D. R. & Turelli, M. *Wolbachia*
776 Acquisition by *Drosophila yakuba*-Clade Hosts and Transfer of Incompatibility Loci
777 Between Distantly Related *Wolbachia*. *Genetics* **212,** 1399–1419 (2019).
778 44. Sinha, A., Li, Z., Sun, L. & Carlow, C. K. S. Complete Genome Sequence of the
779 *Wolbachia* wAlbB Endosymbiont of *Aedes albopictus*. *Genome Biology and*
780 *Evolution* **11,** 706–720 (2019).
781 45. Kautz, S., Rubin, B. E. R. & Moreau, C. S. Bacterial Infections across the Ants:
782 Frequency and Prevalence of *Wolbachia*, *Spiroplasma*, and *Asaia*. *Psyche: A Journal*
783 *of Entomology* **2013,** 1–11 (2013).
784 46. Russell, J. A. *et al.* Specialization and geographic isolation among *Wolbachia*
785 symbionts from ants and lycaenid butterflies. *Evolution* **63,** 624–640 (2009).
786 47. Tolley, S. J. A., Nonacs, P. & Sapountzis, P. *Wolbachia* Horizontal Transmission
787 Events in Ants: What Do We Know and What Can We Learn? *Front Microbiol* **10,**
788 296 (2019).
789 48. Kelly, M., Price, S. L., de Oliveira Ramalho, M. & Moreau, C. S. Diversity of *Wolbachia*
790 Associated with the Giant Turtle Ant, *Cephalotes atratus*. *Curr Microbiol* **76,** 1330–
791 1337 (2019).
792 49. Arnold, P. A., Levin, S. C., Stevanovic, A. L. & Johnson, K. N. *Drosophila*
793 melanogaster infected with *Wolbachia* strain wMelCS prefer cooler temperatures.
794 *Ecological Entomology* **44,** 287–290 (2018).
795 50. Truitt, A. M., Kapun, M., Kaur, R. & Miller, W. J. *Wolbachia* modifies thermal
796 preference in *Drosophila melanogaster*. *Environ Microbiol* **21,** 3259–3268 (2018).
797 51. Coyne, J. A. & Orr, H. A. 'Patterns of speciation in *Drosophila*' revisited. *Evolution*
798 **51,** 295–303 (1997).

52. Schwander, T., Suni, S. S., Cahan, S. H. & Keller, L. Mechanisms of reproductive isolation between an ant species of hybrid origin and one of its parents. *Evolution* **62,** 1635–1643 (2008).
53. Heinze, J. & Hölldobler, B. Fighting for a harem of queens: physiology of reproduction in *Cardiocondyla* male ants. *Proc Natl Acad Sci U S A* **90,** 8412–8414 (1993).
54. Schrempf, A., Darrouzet, E. & Heinze, J. Mating success and potential male-worker conflict in a male-dimorphic ant. *BMC Evol Biol* **7,** 114 (2007).
55. Schmidt, C. V., Frohschammer, S., Schrempf, A. & Heinze, J. Virgin ant queens mate with their own sons to avoid failure at colony foundation. *Naturwissenschaften* **101,** 69–72 (2013).
56. Heinze, J., Cremer, S., Eckl, N. & Schrempf, A. Stealthy invaders: the biology of *Cardiocondyla* tramp ants. *Insect. Soc.* **53,** 1–7 (2006).
57. Seifert, B., Ritz, M. & Csősz, S. Application of exploratory data analyses opens a new perspective in morphology-based alpha-taxonomy of eusocial organisms. *Myrmecological News* **19,** 1–15 (2013).
58. Seifert, B., Okita, I. & Heinze, J. A taxonomic revision of the *Cardiocondyla nuda* group (Hymenoptera: Formicidae). *Zootaxa* **4290,** 324–33 (2017).
59. Campbell, E. A. *et al.* Structural mechanism for rifampicin inhibition of bacterial rna polymerase. *Cell* **104,** 901–912 (2001).
60. Schmittgen, T. D. & Livak, K. J. Analyzing real-time PCR data by the comparative CT method. *Nat Protoc* **3,** 1101–1108 (2008).
61. Bankevich, A. *et al.* SPAdes: a new genome assembly algorithm and its applications to single-cell sequencing. *J. Comput. Biol.* **19,** 455–477 (2012).
62. Wick, R. R., Schultz, M. B., Zobel, J. & Holt, K. E. Bandage: interactive visualization of de novo genome assemblies. *Bioinformatics* **31,** 3350–3352 (2015).
63. Langmead, B. & Salzberg, S. L. Fast gapped-read alignment with Bowtie 2. *Nat Meth* **9,** 357–359 (2012).
64. Seemann, T. Prokka: rapid prokaryotic genome annotation. *Bioinformatics* **30,** 2068–2069 (2014).
65. Ronquist, F. *et al.* MrBayes 3.2: efficient Bayesian phylogenetic inference and model choice across a large model space. *Systematic Biology* **61,** 539–542 (2012).
66. Li, L. OrthoMCL: Identification of Ortholog Groups for Eukaryotic Genomes. *Genome Research* **13,** 2178–2189 (2003).
67. Chen, F., Mackey, A. J., Vermunt, J. K. & Roos, D. S. Assessing performance of orthology detection strategies applied to eukaryotic genomes. *PLoS ONE* **2,** e383 (2007).
68. Kurtz, S. *et al.* Versatile and open software for comparing large genomes. *Genome Biol.* **5,** R12 (2004).
69. Heddi, A., Grenier, A.-M., Khatchadourian, C., Charles, H. & Nardon, P. Four intracellular genomes direct weevil biology: Nuclear, mitochondrial, principal endosymbiont, and *Wolbachia*. *Proceedings of the National Academy of Sciences* **96,** 6814–6819 (1999).
70. Sanguin, H. *et al.* Development and validation of a prototype 16S rRNA-based taxonomic microarray for Alphaproteobacteria. *Environ Microbiol* **8,** 289–307 (2006).

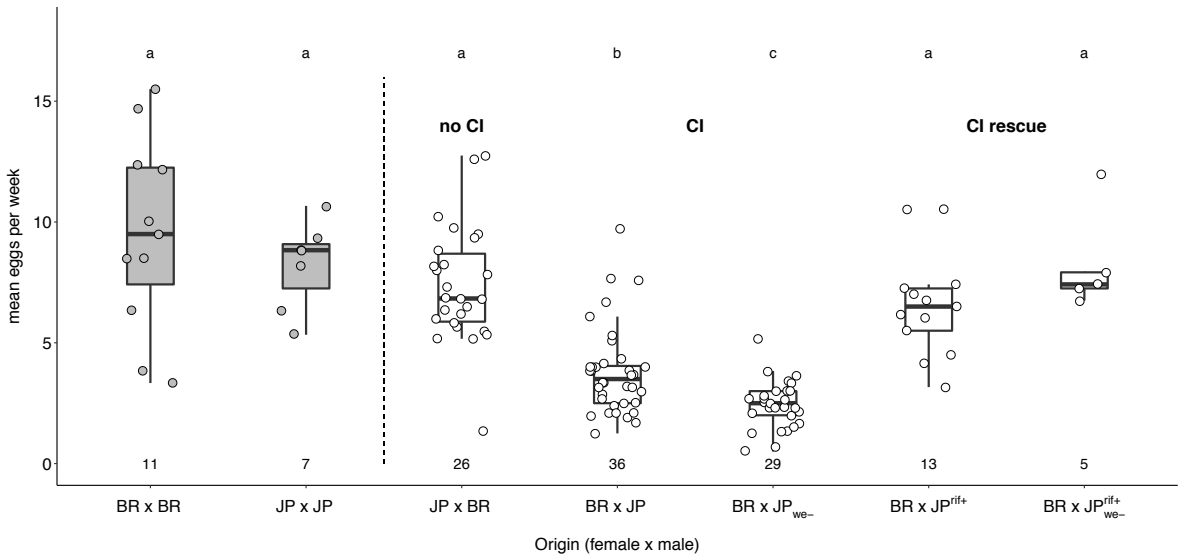

Figure 1: Mean weekly egg numbers produced by intra- and inter-population crosses of the ant *C. obscurior*

Mean weekly egg numbers produced by Brazilian (BR) and Japanese (JP) queens mated to males from their own or from a different population over a period of six weeks. JP ants were collected from colonies that either carried the main endosymbiont *Candidatus* Westeberhardia cardiocondylae (JP) or did not (JP_{we-}). Males used in "CI rescue" crosses were collected from JP colonies with and without *Cand.* Westeberhardia cardiocondylae, which had been treated with the antibiotic rifampicin (JP^{rif+}; JP_{we-}^{rif+}). Numbers below box plots indicate the number of replicates. Differences between groups were tested with pairwise Mann-Whitney-U-tests followed by Bonferroni-Holms correction of p-values. Letters above boxplots indicate statistically significant differences at $p<0.05$. For Bonferroni-Holms corrected pairwise p-values see Table S1.

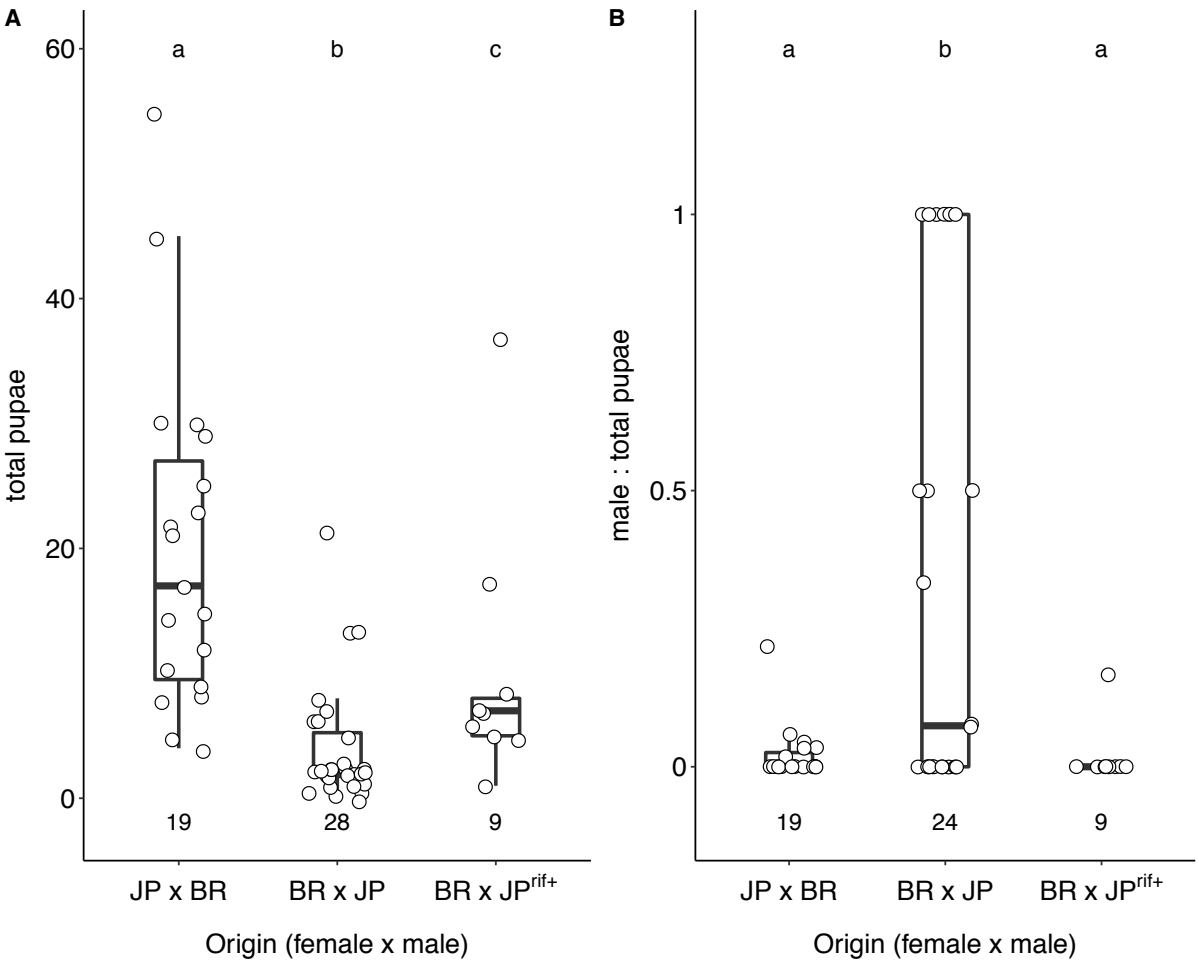

Figure 2: Total pupae numbers and pupae sex ratios produced by intra- and inter-population crosses of the ant *C. obscurior*

Total number of pupae (A) and sex ratio of pupae (B) produced in crosses between Brazilian (BR) and Japanese (JP) queens and males over a period of 12 weeks. All JP ants were collected from colonies that carried the main endosymbiont *Candidatus* Westeberhardia cardiocondylae (JP). Males used in BR x JP^{rif+} crosses were collected from JP colonies that had been treated with the antibiotic rifampicin. Numbers below box plots indicate the number of replicates. For total pupae numbers, differences between groups were tested with pairwise Mann-Whitney-U-tests followed by Bonferroni-Holms correction of p-values. Sex ratios produced by different crosses were compared with a generalized linear model with logit link followed by manual Bonferroni-Holms correction of p-values. Letters above boxplots indicate statistically significant differences at $p<0.05$.

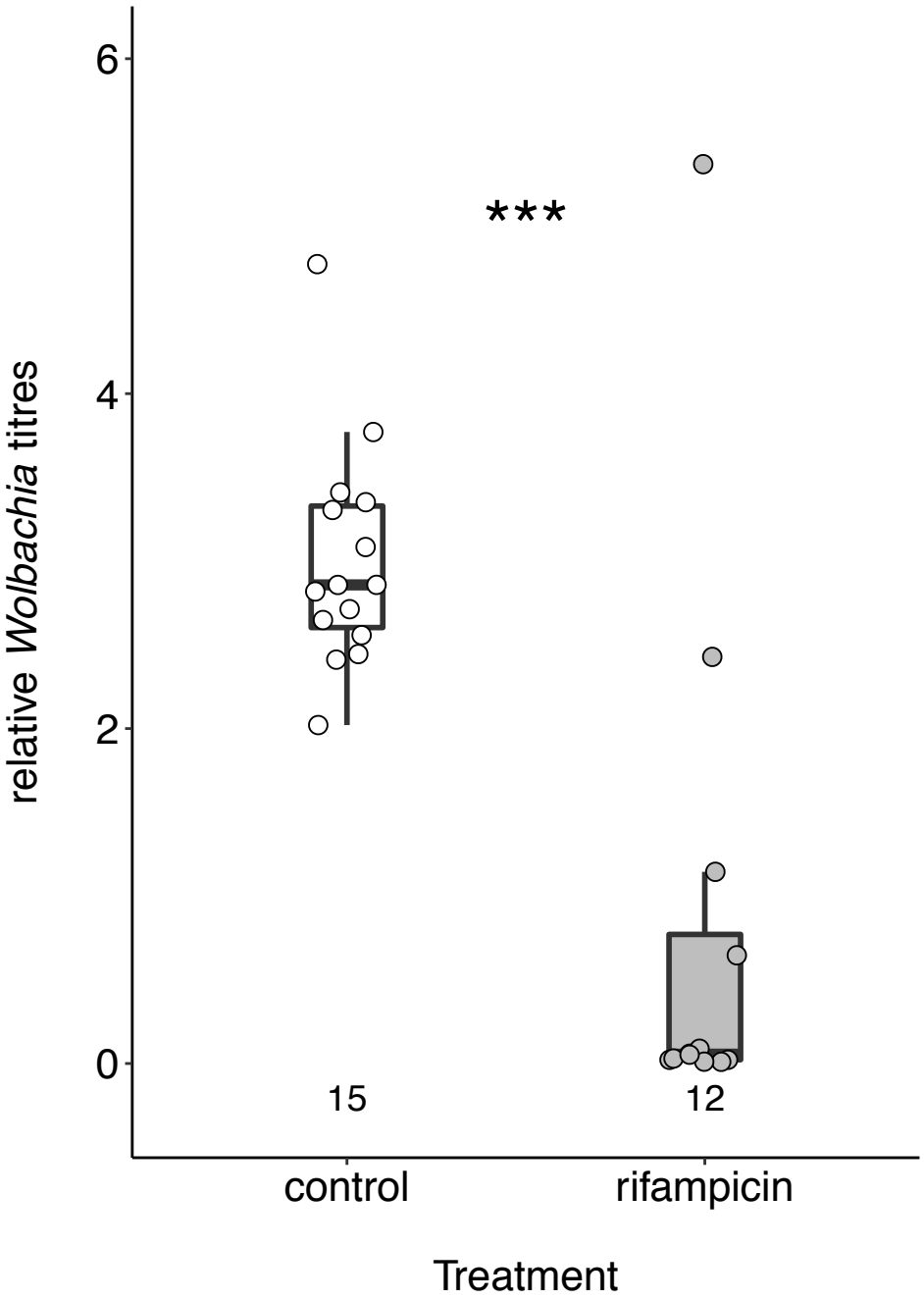

Figure 3: Effects of rifampicin treatment on *Wolbachia* titres in males
All males were collected from colonies that carried the main endosymbiont *Candidatus* Westeberhardia cardiocondylae. Numbers below box plots indicate the number of replicates. Differences in *Wolbachia* titres between control and rifampicin-treated males were tested with a Mann-Whitney-U-Test. Stars indicate statistically significant differences at $p<0.001$ (***).

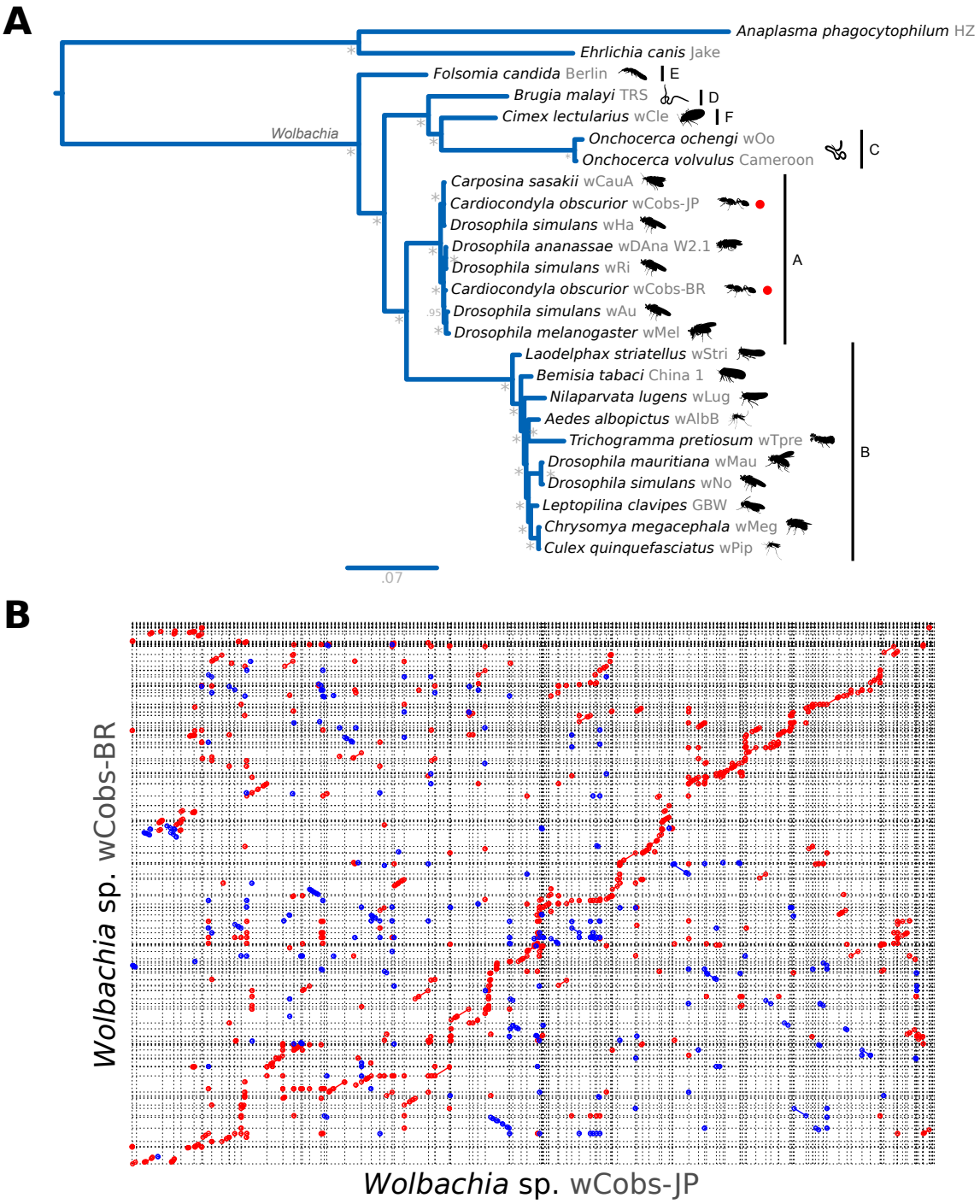

Figure 4: *Wolbachia* spp. phylogeny and genome synteny

(A) Bayesian phylogenetic placement of *Wolbachia* strains sequenced from *C. obscurior* (*w*Cobs-BR and *w*Cobs-JP). *Anaplasma phagocytophilum* and *Ehrlichia canis* were used as outgroups. For *Wolbachia*, names at tips correspond to the host from which they were sequenced/isolated. Red dots are used to highlight the newly sequenced strains. Next to the binomial names, strain names are shown in grey and silhouettes for the host are sketched in black. Horizontal bars delimit *Wolbachia* supergroups (A-F). *=1.0 posterior probability. (B) Genome-wise nucleotide-based synteny plot between *w*Cobs-BR and *w*Cobs-JP. Red is used to indicate a direct match and blue a reverse complement match.

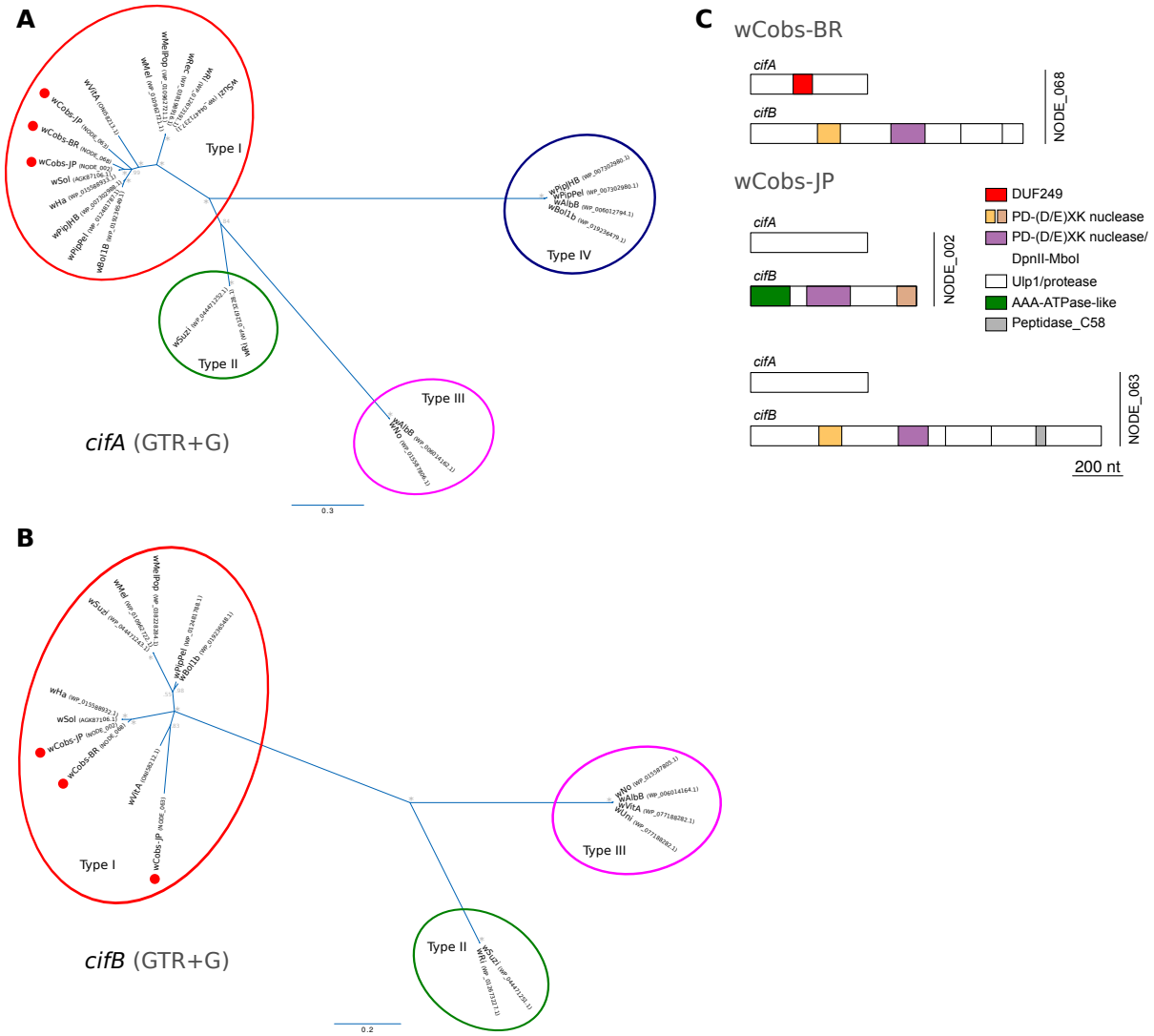

Figure 5. Phylogeny and domain structure of *cif* genes

Bayesian phylogenetic trees for (A) *cifA* and (B) *cifB* genes. Colored ovals are used to highlight the different gene "types". *= 1.0 posterior probability. (C) Domain structure for the *cif* genes of *w*Cobs-BR (top) and *w*Cobs-JP (bottom) strains. For the latter, the two loci are shown and indicated with a vertical bar to the right of the sketches. Color codes and designation of the domains are shown in the legend.

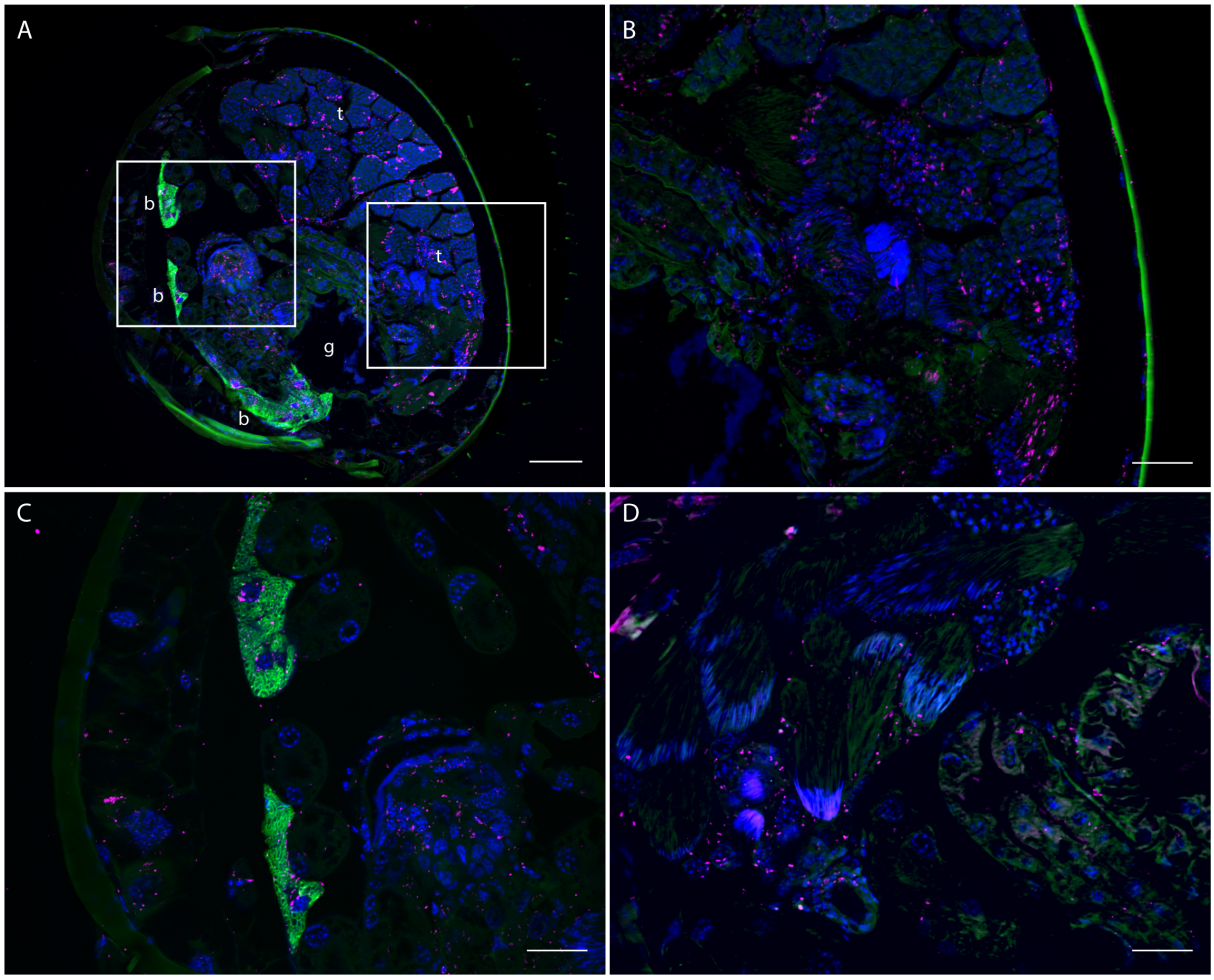

Figure 6: Localization of endosymbiotic bacteria in male adult abdomens of *C. obscurior* via fluorescence in situ hybridization.

Wolbachia were specifically stained with two Cy5-labeled probes (magenta), and *Cand.* Westeberhardia with a Cy3-labeled probe (green). Host cell nuclei are counterstained with DAPI (blue). (A) Transversal section of *C. obscurior* JP male abdomen showing the testes (t), the *Cand.* Westeberhardia-containing bacteriomes (B) and the gut (g). The areas indicated by rectangles are displayed in higher magnification showing *Wolbachia*-infected seminiferous tubules (B) and bacteriomes co-infected with *Cand.* Westeberhardia and *Wolbachia* (C). (D) *C. obscurior* BR male testes and gut epithelium infected with *Wolbachia*. Scale bars: 50 µm (A) and 20 µm (B-D).

Table 1: Wolbachia genome assembly statistics

Genome assembly and draft annotation statistics for the newly sequenced *Wolbachia* strains from *C. obscurior* (*w*Cobs-BR and *w*Cobs-JP).

	Wolbachia	
	wCobs-BR	**wCobs-JP**
Assembled genome size (Mbp)	1.19	1.30
Number of scaffolds	148	182
N50	14,698	16,173
G+C content (%)	35.3	35.1
Predicted CDSs*	1,013	1,058
tRNAs	34	34
rRNAs	3	3
Other ncRNAs genes/motifs	71	54